

# INTERNATIONAL SOCIETY FOR SOIL MECHANICS AND GEOTECHNICAL ENGINEERING



*This paper was downloaded from the Online Library of the International Society for Soil Mechanics and Geotechnical Engineering (ISSMGE). The library is available here:*

<https://www.issmge.org/publications/online-library>

*This is an open-access database that archives thousands of papers published under the Auspices of the ISSMGE and maintained by the Innovation and Development Committee of ISSMGE.*

*The paper was published in the proceedings of the 7<sup>th</sup> International Conference on Earthquake Geotechnical Engineering and was edited by Francesco Silvestri, Nicola Moraci and Susanna Antonielli. The conference was held in Rome, Italy, 17 - 20 June 2019.*

# Computational and experimental study of seismic site effects on Amatrice hill

G. Grelle

*Department of Civil and Environmental Engineering DICEA, University of Roma “Sapienza”, Italy*

R. Maresca

*Department of Sciences and Technologies, University of Sannio, Benevento, Italy*

E. Gargini

*University of Florence, Centro per la Protezione Civile, Florence, Italy*

J. Facciorusso & C. Madi ai

*Department of Civil and Environmental Engineering DICeA, University of Florence, Florence, Italy*

**ABSTRACT:** Amatrice is considered the town symbol of the destructive effects induced by 2016 Central Italy seismic sequence. As a result of the two main shocks (August 24<sup>th</sup>, M=6.0 and October 30<sup>th</sup>, M=6.5) the ancient urban area of the municipality, located on a hilly promontory, was heavily damaged. Old buildings, but also renovated and new buildings, suffered many cracks and collapses. Subsoil geological, geophysical and geotechnical data were collected in the area and seismic data were also available. By using and interpreting the subsoil data, a 3D-GIS model was developed, that is the basic geometrical model for SiSeRHMap hybrid-analysis. Several 2D sections crossing the seismic station sites were extracted from this model and analyzed by 2D-FEM numerical approaches. Comparison of numerical results and seismic experimental data allowed to: i) validate the subsoil model used in the simulations; ii) show the significant role of the topographic effects in the area under study; and iii) point out the variability of the 2D numerical results depending on the direction of the analyzed cross-sections.

## 1 INTRODUCTION

The contribution of site seismic amplification phenomena on damage can be quite different in relation to geo-lithological and geo-morphological features and their combined effect. Moreover, the difficulty in evaluating site seismic effects increases in relation to the complexity of the underground morphology that characterizes the site (Madi ai et al. 2017; Facciorusso et al. 2016, among others) as well as the interaction of these features with the initial wave-form of the regional event.

Following the 2016-2017 Central Italy seismic sequence, field investigations were performed with the aim to define geological, geotechnical and geophysical property for the most damaged area in the town of Amatrice (Red Zone). For this area, the collected data have permitted to define a reliable geotechnical model of the subsoil as well as the ambient vibration behaviour by using HVSR techniques in several sector of the hilly promontory.

The topographic effects in the area were explored by using two computational approaches: a 2D - FEM model and a new generation hybrid model. This latter, called SiSeRHMap (Grelle et al., 2014, 2016), is based on a GIS (Geographic Information System) platform for defining the layering subsoil combined with a DEM-derived (topographic) parameterized model in order to develop multispectral maps, in raster matrix format, regarding the seismic response.

The experimental data allowed to identify the amplification phenomena jointed to the directivity of the predominant shaking and its frequency distribution in relation to the complex geomorphology of the hill.

## 2 STUDY AREA

### 2.1 Geological and topographic features

The Amatrice town rises up on a hilly plateau with an altitude between 850 and 950 meters, at the confluence of Tronto and Castellano rivers; it has an elongated shape with the longitudinal axis oriented on the Apennine direction (NW-SE) and the transversal axis on the anti-Apennine direction (SW-NE). The hilly plateau is structurally supported by the Monti della Laga Unit, and consists of pelitic-arenaceous, subordinately to clayey marly-limestone, lithofacies. This substratum is covered by colluviums or old alluvium deposits in the gentle-slopes/flat-zone or in the valley (Geological Map of Italy, APAT, 1955; Pagliaroli, 2016).

By field surveys collected data regarding geotechnical and geophysical exploration techniques (Figure 1a), it was possible to define in detail the subsoil sequence and geometry that characterizes the Red Zone at the top of the hill. Geophysical investigation and geotechnical in situ and laboratory tests were carried out as part of the activities leading up to Seismic Microzonation of level III in Macroarea 3 - Amatrice (Presidenza del Consiglio dei Ministri - OCDPC n. 394/2016).

The general sequence characterizing the subsoil of Amatrice hill includes a basal rock (ML-h) of sandstone and marly-sandstone/marly-limestone with conglomerate inclusions beginning over a depth of 50-60 m from the ground level and changing at the top to weaker rocks (ML-w) that consist of sandstone and siltstone or a very dense sandy material. Both the deposits are members of the Monti della Laga Units. They are covered by ancient sandy coarse alluvial deposits (AD) extending down to 15-20 meters in depth from the ground level. At the surface, a thin layer of soft deposits of colluvium and/or anthropogenic materials (CD) is present almost everywhere and debris-slope deposits, of the same nature, cover the slopes of the plateau. These deposits are frequently mixed with recent alluvial deposits that constitute the depositional filling material (SD) of both the valleys at the base of the hill and a topographic depression in the southern-west sector. The lithological Units described above were defined with respect to the trend of the shear wave velocity with depth and subsequently geometrically distributed via the GIS semi-automatized procedure of SiSeRHMap models (Figure 1b). From this subsoil model the 2D-cross sections used in the 2D-FEM analysis were extracted.

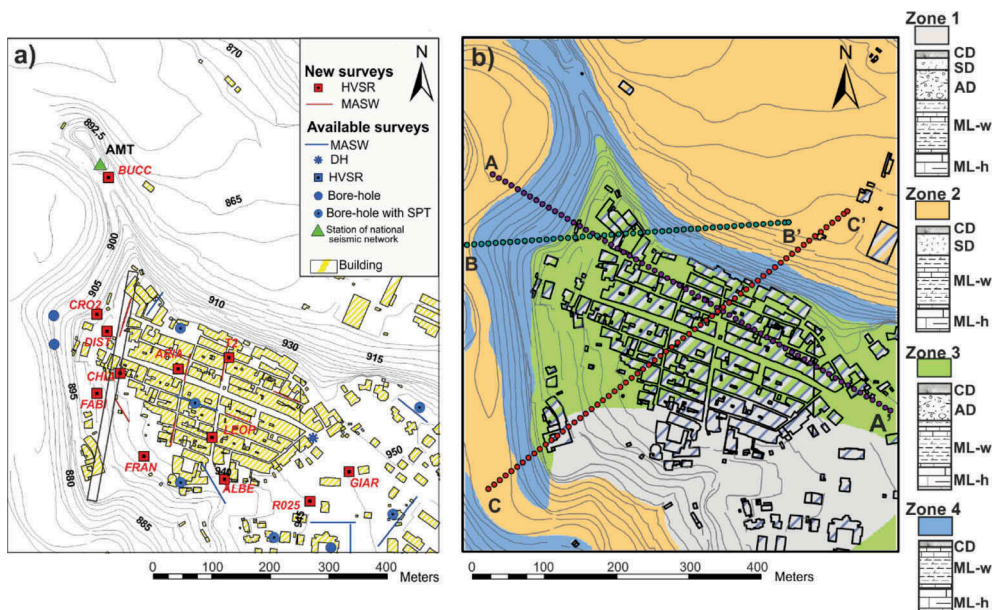


Figure 1. Surveys map and HVSR station sites (a); geo-lithological zonation map obtained by using GIS modeling in SiSeRHMap and cross-sections used in the 2D-FEM analysis (b).

### 3 GEOTECHNICAL MODEL

Three cross-sections of Amatrice area were analysed in this work: the AA' cross section was defined longitudinal to the hilly promontory, while BB' and CC' were defined transversal to the promontory and located close to the ridge and the central zone, respectively (Figure 1b). Free field boundary condition (FFBC) were assumed in performing numerical analyses.

As an example, the model for a representative transversal cross-section with all the five previously described lithological Units and the assumed FFBC is sketched in Figure 2.

#### 3.1 Dynamic soil properties

For the purpose of seismic ground response numerical modelling, each lithological Unit was characterized by means of: density ( $\rho$ ), shear waves velocity ( $V_S$ ), Poisson ratio ( $\nu$ ) and curves of damping ratio ( $D$ ) and shear modulus normalized to initial modulus ( $G/G_0$ ) with shear strain ( $\gamma$ ). The main physical and mechanical properties assumed in the numerical analyses for each lithological Unit are summarized in Table 1. Figure 3 shows the corresponding curves of the normalized shear modulus and damping ratio versus shear strain.

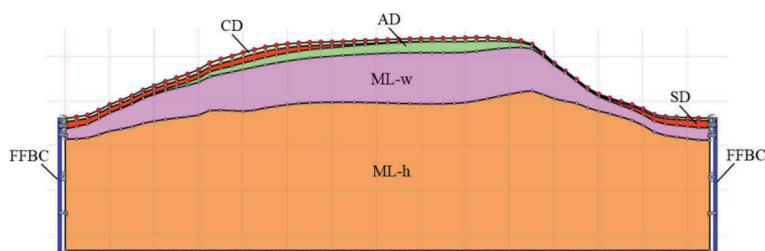


Figure 2. Sketch of a representative transversal cross-section.

Table 1. Main physical and mechanical soil properties.

Lithological Unit	$\rho$ [kg/m <sup>3</sup> ]	$V_S$ [m/s]	$V_P$ [m/s]	$\nu$ [-]	$D_0$ [%]
CD	1800	250	520	0.35	2.2
SD	1800	260	485	0.30	2.2
AD	2000	380	710	0.30	1.0
ML-w	2100	580	1085	0.30	0.5
ML-h	2300	1100	1905	0.25	0.5

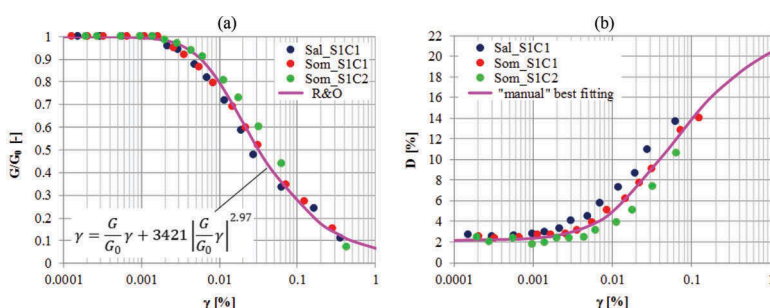


Figure 3. Normalized shear modulus (left) and damping ratio (right) curves.

The shear modulus and damping ratio curves for CD lithological Unit were obtained from Resonant Column (RC) tests performed by the Geotechnical Laboratory of the University of Florence on three soil samples taken from boreholes carried out at two sites located in Saletta and Sommati hamlets in the municipality of Amatrice, where a similar Unit was encountered.

The main characteristics of the tested samples, that are depth ( $z$ ), unit weight ( $\gamma_n$ ), liquid limit ( $w_L$ ), plasticity index (PI) and effective confining pressure ( $\sigma'_c$ ), are summarized in Table 2. Figure 4 shows the curves that best fit the RC experimental data for numerical modelling. Specifically, the Ramberg and Osgood (1943) model was adopted to fit the experimental data for the  $G(\gamma)/G_0$  curve (Figure 4a) whereas the data for the  $D(\gamma)$  (Figure 4b) were fitted ‘manually’ since no literature model gave a satisfactory fitting.

The curves  $G(\gamma)/G_0$  and  $D(\gamma)$  proposed by Vucetic and Dobry (1991) for  $PI=30\%$  were attributed to SD Unit, assuming  $D_0=2.2\%$  based on the experimental values obtained for CD Unit. Modoni and Gazzellone (2010) curves were adopted for AD lithological Unit, while ML-w and ML-h Units referred to the dynamic behaviour of Yellow and Green Tuff (de Silva et al., 2015).

### 3.2 $V_s$ - $z$ profiles

The  $V_s$  profiles for each lithological Unit were derived from the results of DH (Down Hole) and MASW (Multichannel Analysis of Surface Waves) tests, combined with experimental HVSR (Horizontal to Vertical Spectral Ratio) measurements.  $V_p$  profiles were ‘indirectly’ determined by assuming for each Unit a value of the Poisson ratio,  $\nu$ , recommended in literature for comparable soil types.

The shear wave velocity resulting from the geophysical surveys and the normalized Standard Penetration Test (SPT) empirical correlations allowed to distinguish, in the complete sequence, four main litho-dynamic units LU (sensu Grelle et al 2014): ML-w, AD, SD, CD overlying a uniform bedrock (ML-h). The definition of the  $V_s$ -depth( $z$ ) trend associated to each litho-dynamic unit (Figure 5) is the main step to optimize the parametrization of the model subsequently used to perform the simulation analyses by means of SiSerHMap package. Specifically,  $V_s$ -depth relations are defined as  $V_s(z) = V_0 + \alpha \ln(1+z)$  for covering and  $V_s(z) = V_0 + \alpha z$  for bedrock litho-dynamic Unit, respectively, which were determined from the  $V_s$ -depth dataset defined by means of the preliminary association analysis. For all the

Table 2. Main characteristics of the tested samples from CD lithological Unit.

Site	Sample	USCS	$z$ [m]	$\gamma_n$ [kN/m <sup>3</sup> ]	$w_L$ [%]	PI [%]	$\sigma'_c$ [kPa]
Saletta	Sal_S1C1	CL	2.0 ÷ 2.5	19.82	30	14	80
Sommati	Som_S1C1	CL	2.5 ÷ 3.0	20.60	24	16	80
	Som_S1C2	CL	5.5 ÷ 6.0	19.64	27	18	110

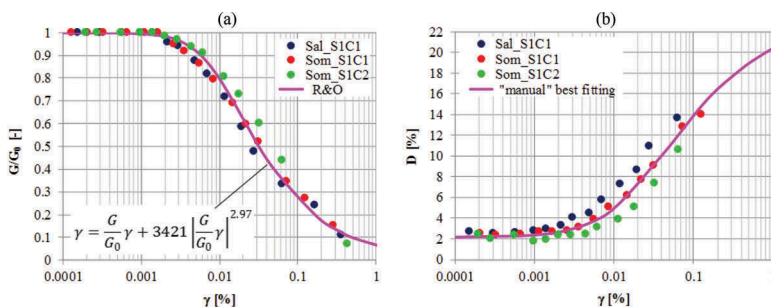


Figure 4. Resonant Column experimental data from CD lithological Unit samples and best fitting  $G/G_0$ - $\gamma$  (a) and  $D$ - $\gamma$  (b) curves.

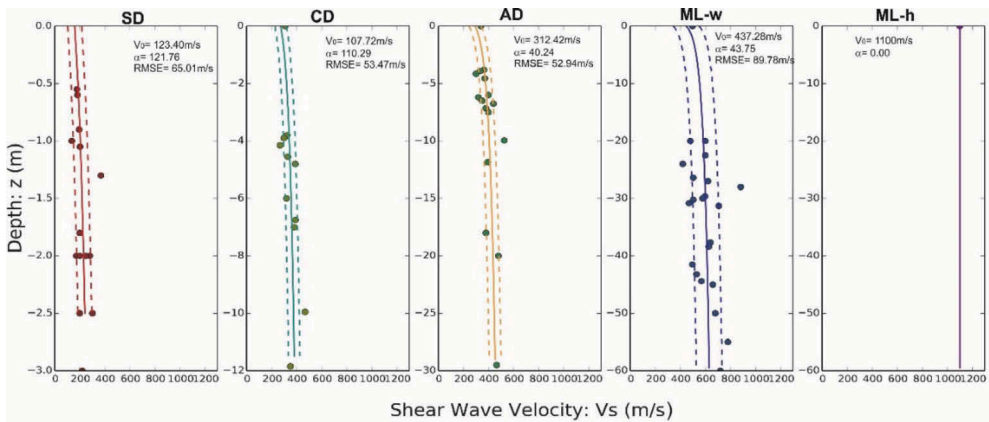


Figure 5.  $V_s$ - $z$  profiles obtained in pre-processing field data by module 1 of SiSeRHMap.

litho-dynamic units of the covering materials, the obtained distributions of the  $V_S(z)$  values point out a good correlation of data by showing Root Mean Square Error (RMSE) values less than 20%. The shear wave velocity of 1100 m/s associated to the bedrock (ML-h) can be considered a median of the metadata values obtained at the end of the seismostratigraphic sequence in the HVSR inversion analyses; this value is also supported by the DH measurements.

#### 4 HVSR ANALYSES

In order to define the spectral distribution of the amplifications by using experimental data, the HVSR tests were performed in sites located at the top of the hill. In this study n. 12 HVSR located within the Red Zone were considered. Triaxial single-station measurements were acquired with a time-windows of 40 minutes and they were processed with the Dinver software (Wathelet et al., 2008). The experimental HVSR curves were then interpreted as the ellipticity of Rayleigh waves. The frequency of the ellipticity peak contains pertinent information about the thickness and the S-wave velocity above the seismic-bedrock.

The polarized analysis was performed in order to highlight the influence of both the azimuthal disposition of the hill and the directionality of the prevailing amplitude of the vibration (Figure 6). From this analysis it was possible to ascertain that some stations (e.g. ALBE, CHIA, FABI, FRAN, SUOR, T2) show clear peaks around 2-3Hz with polarity ranging between 20° and 60°N. These values can be considered variable around the orthogonal direction of the Amatrice hilly dorsal (N125°E). This effect is confirmed and increased when the spectral ratio analysis is performed on the seismic weak motion data (aftershocks acquired by permanent seismic stations), rather than the seismic noise data. The study is in progress; it should be the object of a next paper but it will be brought into discussion during the ICEGE conference.

### 5 COMPUTATIONAL ANALYSES AND RESULTS

#### 5.1 2D-FEM analysis

The 2D ground response analyses were performed by means of LSR2D (STACEC, 2017), a time domain equivalent linear computer program that implements the Finite Element Method and perform numerical analyses in total stress for elastic bedrock conditions. The analysis domain was subdivided into triangular elements to better define morphological and topographic irregularities and boundaries. To allow to transfer the highest frequency  $f_{max}$  of the input motion that is considered as significant (20Hz), the maximum dimension  $\Delta h$  of the triangular finite elements within each soil layer was assumed according to the Kuhlemeyer and Lysmer (1973) relationship.

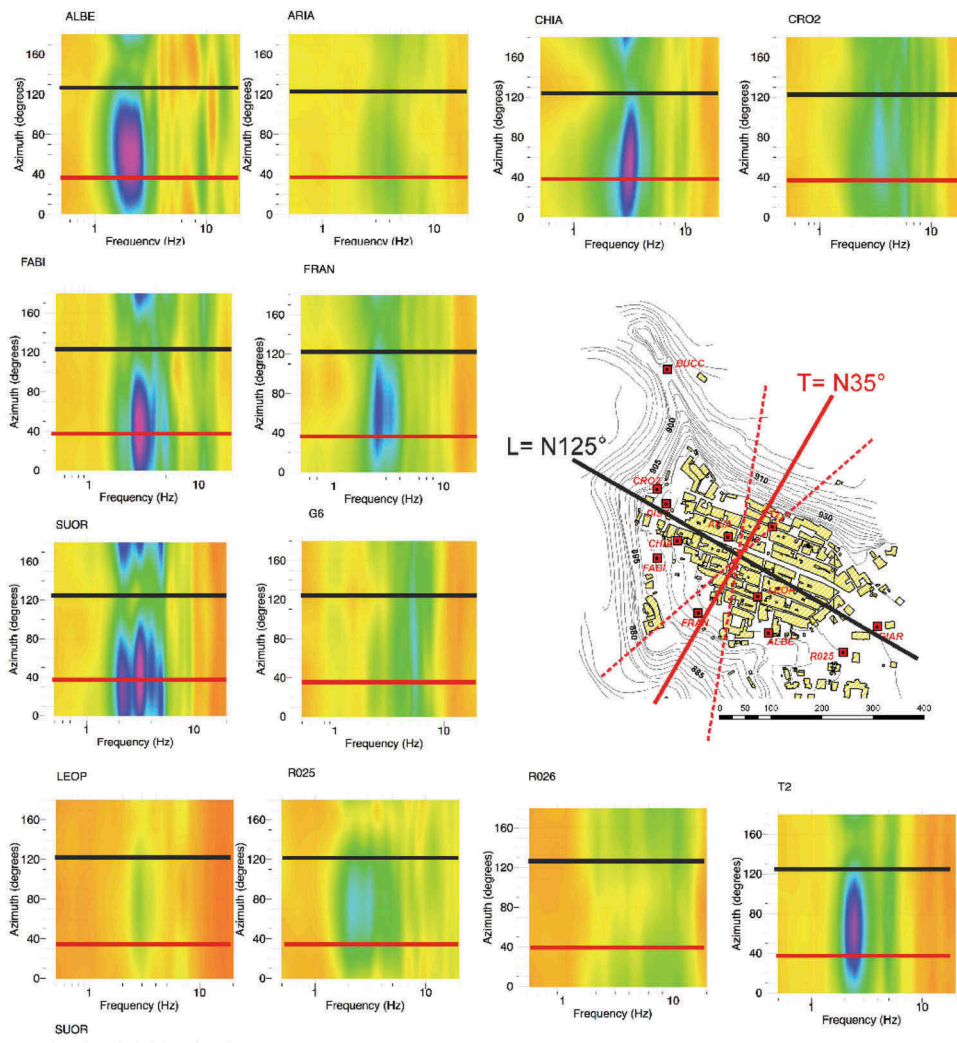


Figure 6. HVSr directional analysis.

The seismic input motion represented by vertically incident SV shear waves and P compression waves is applied simultaneously to all the boundary nodes at the base of the analysis domain and the equation system is solved in the time domain using the CAA method (Constant Average Acceleration Method). Free-field conditions are considered at the lateral boundaries by using normal and tangential viscous dampers connecting the lateral boundary nodes of the analysis domain to as many nodes of appropriate free-field soil columns (Figure 2).

### 5.2 Hybrid model analysis by SiSeRHMap

SiSeRHMap (Grelle et al., 2016) is a Python–Computer Code, composed of five different modules, which uses the Geographic Information System (GIS) data-layers to produce multispectral maps of damped acceleration response. The litho-dynamic units LU composing the layered subsoil, the zones defined by vertical profiles obtained combining LU’s with the Digital Elevation Model and the derived morphometric parameters constitute the key elements in the modelling. The basis of the code is a general model that considers the coupled stratigraphic and topographic effects in the same way as a “serial-parallel physical system” (Grelle et al 2018). In this

system, the 1D seismic wave propagation is analysed by using a viscoelastic model solved in the frequency domain in terms of total stresses applying a linear equivalent approach. The analysis is performed on a given number of possible Vs-profiles chosen with uniform probability in each zone (Figure 1b). The results allow to train a dedicated metamodel that, solved in each cell, permits to obtain maps of damped acceleration response spectra. After that, the stratigraphic acceleration response spectra are scaled at each frequency by an appropriate Topographic Aggravation Factor (TAF) value (serial mode) which is obtained from a heuristic model that takes into account the morphometric shape of the relief and the stiffness of the constituting materials (parallel mode).

The TAF values are obtained by resolving a grey box model which is frequency and 3D-spatial surface dependent. The model is composed of two non-linear functions matching in trend the solution of the regular uniform bi-dimensional Geli's half relief (Geli et al. 1988). The two functions are respectively solved on the slope and on the ridge sector on the basis of a Digital Elevation Model (DTM) with 30m of resolution and its derived parameters as well the slope and curvature digital map values.

### 5.3 Input motion

The input motion used in the simulation consists of the NS horizontal component of the 24<sup>th</sup> August event recorded at the AMT station (Figure 1a). The NS component of the event was chosen in order to consider the lowest topographic effect induced by the morphology of the site because the short elongate hill, where the station is located, shows a nearly E-W transversal direction. The input motion was obtained by 1D deconvolution at the outcrop reference rock by considering the Vs-depth(z) profile extracted from the GIS model of SiSeRHMap at the AMT site where geophysical data surveys were available.

### 5.4 Results and comparisons

The values obtained from the multispectral maps provided by SiSeRHMap were compared to the results from 2D-FEM analyses (Figure 7). In general terms, the comparison shows that the values of the spectral acceleration,  $S_a$ , from the hybrid model are greater than those from the FEM computation (approximately over 30%), but a major gap occurs on the border ridges

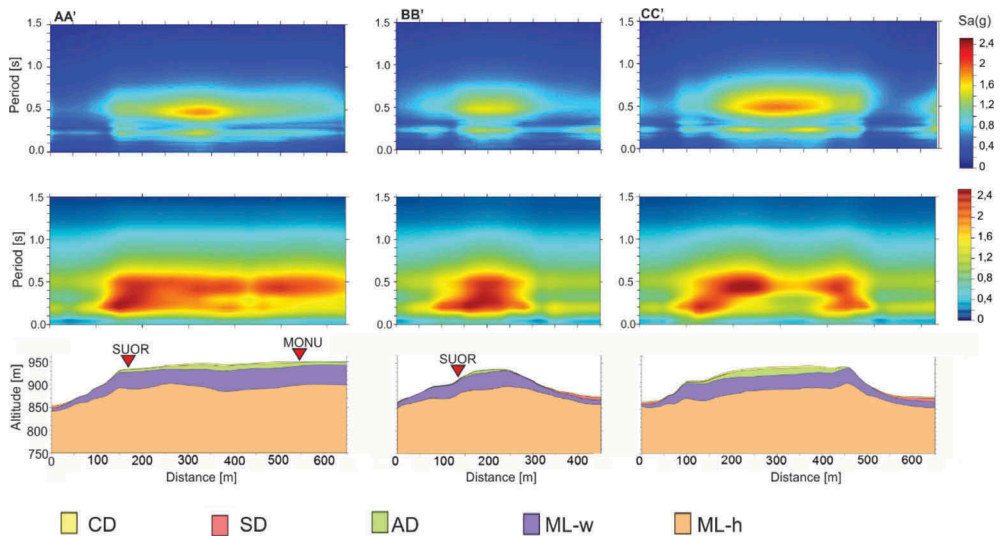


Figure 7. Results from 2D-FEM (top) and hybrid analysis (middle) on the analysed cross-sections (bottom) in terms of spectral acceleration  $S_a$  vs period along the three analyzed cross-sections.

rather than on the central hill. In those sites, the greater values that occur at short periods are attributable to the topographic effect detected by the greater curvature values which refer to the scattering half-wavelength that envelops the slope changing surfaces with a period range of approximately 0.2-0.3s ( $\lambda/2 \sim 60\text{-}100\text{m}$ ) by considering the shear velocity of the uniform relief having a value of 645m/s. With regards to the central sector,  $S_a$  values from the two computational models are comparable to each other with the maximums that refer to about 0.4s.

The greatest difference is shown for the longitudinal cross-section AA', where the 2D-FEM analysis does not show high amplifications near to the ridge. In contrast, the same computational model predicts a substantial increasing of the  $S_a$  values on the ridge if the transversal cross-sections CC' is considered. This difference between the results from the two computational approaches is due to the fact that SiSeRHMap computing is independent from the assumed direction since the TAF spectral maps are computed in terms of maximum possible values based on the minor curvature radius of the ground surface, independently from the local orientation. Consequently, the topographic effect induced by the near orthogonal ridge are also included on the longitudinal section AA'.

## 6 CONCLUSIONS

The experimental and computational analyses have highlighted the significant role of the topographic effect on the seismic response in the Amatrice hilly promontory. In particular, the HVSR analysis shows a remarkable polarization of the spectral peaks in some stations located at the top of the hill. The azimuthal trend of the greatest amplification is observed in the range N20°-60°E. This orientation results coherent with the orthogonal direction (around N120°-130°E) corresponding to the morphometric elongation of the hill in the specific Red Zone sector.

These effects are also confirmed by the results of the computational analyses which highlight a significant amplification at the top of the hill compared to the valleys. In addition, the high values computed by the hybrid model are referred to the ridge sector around the promontory rather than the central sector of the hill where, in contrast, the 2D-FEM analysis has shown the greatest values. In addition, when the 2D analysis is used, the seismic response can be affected by the direction of the cross-section assumed in the computation. Substantial differences in the results occurred mainly in area characterized by a high topographic three-dimensional complexity.

## REFERENCES

- de Silva, F., Ceroni, F., Sica, S., Pecce, M. R. & Silvestri F. 2015. Effects of soil-foundation-structure interaction on the seismic behavior of monumental towers: the case study of the Carmine Bell Tower in Naples. *Rivista Italiana di Geotecnica, Special Edition "Il ruolo della geotecnica nella salvaguardia dei monumenti e dei siti storici"*, 2015.
- Facciorusso, J., Madiari, C. & Vannucchi, G. 2016. The 2012 Emilia earthquake (Italy): Geotechnical characterization and ground response analyses of the paleo-Reno river levees. *Soil Dynamics and Earthquake Engineering*, 86: 71–88.
- Geli, L., Bard, P.Y. & Jullien, B. 1988. The effect of topography on earthquake ground motion: A review and new results. *Bull. of Seismological Society of America*, 78 (1): 42–63.
- Grelle, G., Bonito, L., Lampasi, A., Revellino, P., Guerriero, L., Sappa, G. & Guadagno, F.M. 2016. SiSeRHMap v1.0: a simulator for mapped seismic response using a hybrid model. *Geosci. Model Dev.*, 9: 1567–1596.
- Grelle, G., Bonito, L., Revellino, P., Guerriero, L. & Guadagno F.M. 2014. A hybrid model for mapping simplified seismic response via a GIS-metamodel approach. *Nat. Haz. Earth. Syst. Sci.*, 14: 1703–1718.
- Grelle, G., Wood, C., Bonito, L., Sappa, G., Revellino, P., Rahimi, S. & Guadagno F.M. 2018. A reliable computerized litho-morphometric model for development of 3D maps of Topographic Aggravation Factor (TAF): the cases of East Mountain (Utah, USA) and Port au Prince (Haiti). *Bulletin of Earthquake Engineering*, 16 (5): 1725–1750.
- Kuhlemeyer, R.L. & Lysmer, J. 1973. Finite element method accuracy for wave propagation problems. *J. Soil Mech. Found. Eng. Div. ASCE* 99 (SM5): 421–427.

- Madiati, C., Facciorusso, J. & Gargini, E. 2017. Numerical modeling of seismic site effects in a shallow alluvial basin of the Northern Apennines (Italy). *Bulletin of the Seismological Society of America*, 107 (5): 2094–2105.
- Modoni, G. & Gazzellone, A. 2010. Simplified theoretical analysis of the seismic response of artificially compacted gravels. *Proc. 5th International Conference on Recent Advance in Geotechnical Earthquake Engineering and Soil Dynamics*, San Diego (California), paper #1.28.a.
- Pagliaroli, A. 2016. Terremoto Italia Centrale del 24 agosto 2016: valutazione preliminare degli effetti di sito. *Università di Chieti e Pescara "G. d'Annunzio"*, 14 ottobre 2016. doi: 10.13140.
- Ramberg, W. & Osgood, W. R. 1943. Description of stress–strain curves by three parameters. *Technical Note No. 902, National Advisory Committee for Aeronautics*, Washington DC.
- STACEC s.r.l. 2017. LSR 2D (Local Seismic Response 2D). *User Manual*. <http://www.stacec.com>.
- Vucetic, M. & Dobry, R. 1991. Effect of soil plasticity on cyclic response. *Journal of Geotechnical Engineering*, 117 (1): 87–107.
- Wathelet, M., Jongmans, D., Ohrnberger, M., & Bonnefoy-Claudet S. 2008. Array performances for ambient vibrations on a shallow structure and consequences over Vs inversion. *J. of Seism.*, 12: 1–19.